

---

# ELECTROCATALYST DISCOVERY THROUGH TEXT MINING AND MULTI-OBJECTIVE OPTIMIZATION

---

**Lei Zhang**

Interdisciplinary Centre for Advanced Materials Simulation  
Ruhr-University Bochum  
Universitätsstraße 150  
44780 Bochum, Germany  
lei.zhang-w2i@rub.de

**Markus Stricker**

Interdisciplinary Centre for Advanced Materials Simulation  
Ruhr-University Bochum  
Universitätsstraße 150  
44780 Bochum, Germany  
markus.stricker@rub.de

March 3, 2025

## ABSTRACT

The discovery and optimization of high-performance materials is the basis for advancing energy conversion technologies. To understand composition-property relationships, all available data sources should be leveraged: experimental results, predictions from simulations, and latent knowledge from scientific texts. Among these three, text-based data sources are still not used to their full potential. We present an approach combining text mining, Word2Vec representations of materials and properties, and Pareto front analysis for the prediction of high-performance candidate materials for electrocatalysis in regions where other data sources are scarce or non-existent. Candidate compositions are evaluated on the basis of their similarity to the terms ‘conductivity’ and ‘dielectric’, which enables reaction-specific candidate composition predictions for oxygen reduction (ORR), hydrogen evolution (HER), and oxygen evolution (OER) reactions. This, combined with Pareto optimization, allows us to significantly reduce the pool of candidate compositions to high-performing compositions. Our predictions, which are purely based on text data, match the measured electrochemical activity very well.

## 1 Introduction

Electrocatalysts are essential components in energy conversion technologies, such as fuel cells [1, 2, 3, 4], water electrolyzers [5, 6, 7], and metal-air batteries [8, 9, 10]. These technologies are critical for transitioning to a clean energy future, as they enable efficient energy storage and conversion without reliance on fossil fuels. At the heart of these technologies are reactions such as the oxygen reduction reaction (ORR) [11, 12, 13], hydrogen evolution reaction (HER) [14, 15], and oxygen evolution reaction (OER) [16, 17]. Each of these reactions plays an important role in processes like electricity generation and hydrogen production, but their efficiency depends on the performance of the electrocatalysts involved. Developing high-performance, cost-effective electrocatalysts is therefore the basis for viable use cases.

However, the discovery and design of new electrocatalysts presents significant challenges. Electrocatalysts are often composed of multiple elements [18, 19], and their performance is influenced not only by the presence of specific elements but also by their precise proportions and interactions [20, 21]. This creates a practically infinite search space, where the number of possible compositions far exceeds what can be screened experimentally. In addition,

each reaction type poses unique requirements. For example, ORR and HER demand materials with high electrical conductivity [22, 23] to support fast charge transfer, while OER benefits from materials with higher dielectric properties to promote oxygen evolution [24, 25]. Balancing these often-opposing properties further complicates the search for optimal reaction-specific materials.

Traditional methods for the discovery of electrocatalysts are based on trial and error experiments [26, 27]. Researchers typically test individual compositions one at a time, measuring their performance under specific conditions. Although this approach has led to many important breakthroughs, it is slow, expensive, and inefficient, particularly as the (compositional) complexity of material systems grows. Even high-throughput approaches alone can not tame the ‘combinatorial explosion’ to tune and optimize the precise compositions and make use of the available design space [28]. Therefore, many potentially promising materials remain untested, either because they are overlooked or because testing every possibility is simply impractical. This represents a bottleneck in the discovery and optimization of future energy technologies.

Experimental data is precious because it is expensive to obtain even in high-throughput, automated labs. Quantum-accurate simulations also require many calculations in quaternary or quinary composition spaces when high resolution in composition space is required [29]. Knowledge in scientific texts, however, exists. The challenge is how to use it effectively. Thousands of scientific articles are published every year that contain potentially valuable data and insights on material properties, synthesis methods, and performance metrics. However, this information is scattered and difficult to integrate into a cohesive *picture* to establish composition-property relationships. The lack of systematic methods to extract and leverage this knowledge has probably left many materials underexplored or just overlooked. Bridging this gap requires tools that can process and analyze large volumes of scientific literature and models that use this information to establish correlative structure-property relationships.

Advances in data science, particularly natural language processing (NLP) [30, 31] and machine learning [32, 33, 34], offer promising solutions to these challenges. NLP techniques can process large amounts of text, e.g. a corpus of research articles, extracting correlations between material compositions, properties, and performance metrics, e.g. in the form of word embeddings. Word embeddings, like those generated by Word2Vec models, encode complex materials-specific terms as numerical representations amenable for model development and optimization. The relationship between composition and property vectors enables quantitative comparisons that can be used predictively [35]. These techniques not only automate the extraction of latent knowledge from text but also provide a way to link material representations to measurable properties [36] like conductivity or dielectric behavior (polarizability), purely based on the probability of co-occurrence of words as they are presented in scientific texts. Such links enable the evaluation of potential applications of a material prior to any experimental measurement, thereby opening the door to systematically accelerate material discovery.

Our study introduces an approach that combines automated text mining, Word2Vec models, and Pareto optimization to filter likely high-performing candidate compositions from a large number of possible compositions for application in the three electrocatalytic reactions mentioned above. Text mining extracts relevant information from open-access abstracts; Word2Vec models are used to generate embeddings for the calculation of similarity scores for key properties. These scores are then used in Pareto optimization to filter large datasets for best-performing candidate materials. Our approach reduces experimental workload by leveraging reaction-specific Pareto optimization directions tailored to ORR, HER, and OER. By linking qualitative descriptions from scientific literature to quantitative optimization, our method offers a scalable framework for accelerated materials discovery and optimization.

## 2 Methods

We describe in detail our workflow in the following: From the collection of open-access abstracts of scientific articles, Word2Vec model building, Pareto front calculation. All code to reproduce our findings or reuse our approach is publicly accessible and licensed under LGPL in Version 3.0 [37].

### 2.1 Automated Paper Collection

To create a Word2Vec embeddings [38, 39], abstracts related to electrocatalysts and high-entropy alloys are collected using the `PaperCollector` module in `MatNexus` [35]. The sources of these abstracts are Scopus and ArXiv. In our study we only include only open-access publications. To keep the data set comprehensive and up-to-date, the query includes all relevant publications up to the year 2024. The query includes automated retrieval of bibliographical metadata along with the respective abstracts. The collected data is then saved in a structured CSV format before further processing.

## 2.2 Text Processing

Text processing uses the `TextProcessor` module of `MatNexus`. This step preprocesses the collected raw abstracts for natural language processing by cleaning and organizing the text.

*Cleaning* and filtering comprises:

- **Removing unnecessary content:** Parts of the text containing “©” or “& Co.” are removed to exclude licensing information and publisher-specific content.
- **Filtering out common words:** Standard English stopwords are removed to reduce noise, ensuring that only meaningful words are kept.
- **Extracting chemical information:** Chemical element symbols and formulas are identified and kept, as they are key to establishing composition-property relationships in word embedding space.

The cleaned text is tokenized and saved in a structured format, ready for model training.

## 2.3 Word2Vec Model Training

To train a Word2Vec model [38, 39], we use the `VecGenerator` module in `MatNexus`. Compared to other word vector training methods, such as count-based embeddings or TF-IDF, Word2Vec generates dense vectors that represent words in a continuous vector space, allowing for an assessment of the correlations of terms which is important for our method. Unlike methods that rely solely on word co-occurrence frequencies, Word2Vec considers the context within sentences: words appearing in similar contexts are mapped to close-by vector representations measured by cosine similarity. More advanced techniques like transformers (e.g., BERT or GPT) for understanding text exist; however, they require significantly larger computational resources and training datasets to perform effectively, which can be a limiting factor when working with domain-specific corpora like ours. Additionally, transformers are often overparameterized for tasks such as word embedding generation, where simpler models such as Word2Vec are sufficient to capture the essential relationships [40]. Given the specific goal of creating word embeddings to support material discovery, we chose Word2Vec for its balance between computational efficiency and accuracy for our scenario.

For training, we selected the following parameters:

- **Model type:** Skip-gram was used to capture contextual relationships in texts.
- **Vector size:** The word vectors were set to 200 dimensions to represent the information.
- **Training method:** Hierarchical softmax was used to handle large vocabulary.
- **Context window:** A window size of 5 words was used to capture local relationships between terms.
- **Minimum word frequency:** Words appearing at least once were included to maximize the dataset’s coverage.
- **Parallel processing:** Multiple threads were used to for training efficiency.

The processed abstracts are used to train the Word2Vec model with these settings to create word embedding-based representations for downstream analysis.

## 2.4 Dataset Preparation and Similarity Calculation

The dataset preparation process involves loading a pre-trained Word2Vec model as per the previous explanation. With this we calculate material similarities for target properties such as ‘dielectric’ and ‘conductivity’. These properties were chosen for their relevance to the study of electrocatalysts and high-entropy alloys [41].

The input data consisted of many different compositions for different material systems. ‘Material system’ refers to a fixed number elements. Within one material system, only the concentration (composition) varies. For each specific composition, similarity scores w.r.t. the target properties are calculated using the Word2Vec model. The resulting similarity scores indicate how *similar* the embedding representation of a specific compositions is with a selected property. Similarity scores are then used as features for each composition for the Pareto front optimization as per the following step.

## 2.5 Pareto Front Calculation

The Pareto front method is a widely used multi-objective optimization technique that identifies solutions offering the best trade-offs between conflicting objectives [42]. This method has been applied in various fields, such as materials

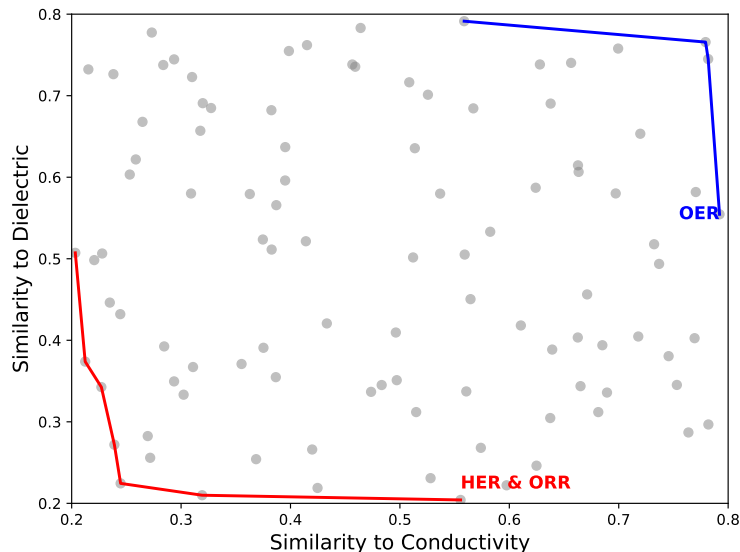


Figure 1: Pareto front visualization depicting trade-offs between similarity to conductivity and dielectric properties.

design and engineering [43, 44], where multiple competing goals are optimized. In Pareto optimization, a solution is considered non-dominated if no other solution performs better in all objectives simultaneously. By focusing on non-dominated solutions, Pareto optimization narrows the search space to candidates that strike a balance between the objectives, enabling decision-making in complex systems. We use Pareto front optimization to identify optimal trade-offs between material properties tailored for specific reactions: hydrogen evolution reaction (HER), oxygen reduction reaction (ORR), and oxygen evolution reaction (OER). The objectives and optimization directions were defined based on the reaction type, reflecting the opposing nature of these processes.

Fig.1 schematically illustrates the Pareto front for HER/ORR and OER w.r.t the similarity of compositions with the terms ‘conductivity’ and ‘dielectric’. Gray points represent randomly generated data points for the two similarities. For HER and ORR, the goal is to maximize similarity to ‘conductivity’ and minimize similarity to ‘dielectric’ (red line), as high conductivity and low dielectric properties are desirable [22, 23]. In contrast, for OER, the goal is to minimize similarity to ‘conductivity’ and maximize similarity to ‘dielectric’ (blue line) [24, 25]. For each material system, we create such a dielectric-conductivity-similarity space. Within each of these spaces, the compositions on the Pareto front are our prediction of promising compositions suggested for experimental validation.

## 3 Results

### 3.1 Overview of the Datasets

We investigate six different material systems from the class of compositionally complex solid solutions (a.k.a. high-entropy alloys) [19]. These systems are classified in three groups for the three reaction types: the oxygen reduction reaction (ORR), hydrogen evolution reaction (HER), and oxygen evolution reaction (OER). The ORR group contains the AgPdPt, AgPdRu, and AgPdPtRu systems, the HER group contains the two systems AgAuPdPtRh and AgAuPdPtRu, and the OER group OER group is represented by the NiPdPtRu system. In the following, we present an overview of the experimentally-measured datasets along our predictions for each reaction type along our predictions.

### 3.2 Results for ORR Systems

#### 3.2.1 Elemental Composition

Table 1 provides a statistical overview of the ORR systems for both the original variance in the data as well as the variance of our Pareto-optimal predictions. A full version of the experimental dataset is published on Zenodo [45]. The compositions at the Pareto front exhibit a much narrower range of elemental concentrations compared to the original datasets. For instance:

Table 1: Comparative elemental composition in % across systems: all compositions considered and Pareto-optimal compositions.

System	Element	Max (Original)	Max (Pareto)	Min (Original)	Min (Pareto)	Std Dev (Original)	Std Dev (Pareto)
AgPdPt	Pt	68	58	17	41	13.136	6.01
	Pd	46	44	0	40	12.732	1.57
	Ag	69	14	1	1	17.097	4.439
AgPdRu	Pd	86	86	22	65	16.448	7.934
	Ag	40	14	9	9	7.808	1.242
	Ru	45	22	0	0	12.393	8.484
AgPdPtRu	Pt	56	55	0	50	14.901	2.928
	Pd	27	24	0	21	7.325	1.753
	Ag	39	12	3	7	9.299	2.422
	Ru	67	17	7	10	15.388	3.589
AgAuPdPtRh	Pt	23	21	2	5	5.284	6.889
	Rh	38	38	5	6	8.219	15.751
	Pd	37	36	6	7	8.463	13.69
	Au	52	25	9	19	11.447	2.645
	Ag	45	28	7	14	10.081	6.074
AgAuPdPtRu	Pt	42	34	7	24	9.392	3.017
	Pd	45	43	10	38	9.061	1.785
	Au	15	9	2	6	3.259	1.154
	Ag	25	7	3	5	5.309	0.741
	Ru	61	16	12	12	13.384	1.518
NiPdPtRu	Pt	90	13	0	0	25.543	2.426
	Pd	89	10	0	0	25.749	1.771
	Ni	80	80	0	5	18.511	17.727
	Ru	94	94	0	8	26.098	20.515

Table 2: Measured current densities (mA/cm<sup>2</sup>) and statistical details for electrocatalysts under specified potentials

System	Potential (mV)	Max (Original)	Max (Pareto)	Min (Original)	Min (Pareto)	Mean (Original)	Mean (Pareto)	Std Dev (Original)	Std Dev (Pareto)
AgPdPt	850	-0.063	-0.415	-0.583	-0.447	-0.342	-0.430	0.098	0.011
AgPdRu	850	-0.065	-0.364	-0.673	-0.673	-0.278	-0.463	0.114	0.086
AgPdPtRu	850	-0.060	-0.361	-0.366	-0.366	-0.159	-0.362	0.074	0.003
AgAuPdPtRh	-300	-0.688	-0.982	-1.128	-1.085	-0.892	-1.037	0.098	0.043
AgAuPdPtRu	-300	-0.794	-1.343	-1.494	-1.437	-1.333	-1.395	0.107	0.030
NiPdPtRu	1700	6.896	6.896	0.237	0.756	1.073	3.265	0.843	1.633

- In the AgPdPt system, the maximum concentration of Pt reduced from 68 % to 58 %, while the minimum increased from 17 % to 41 %. This suggests that high-performing candidates favor a balanced composition of Pt.
- For AgPdRu, the minimum concentration of Pd increased significantly from 22 % to 65 %, suggesting its importance for ORR activity.

### 3.2.2 Current Density Metrics

Fig. 2, 3, and 4 present the measured current density and similarity scores distribution for the AgPdPt, AgPdRu, and AgPdPtRu systems, respectively. Each figure consists of three panels: (a) shows the distribution of current density values, while (b) and (c) display the distribution of similarity scores to ‘dielectric’ and ‘conductivity’, respectively.

- **Panel (a):** The original dataset (blue) exhibits a broad distribution of current densities, ranging from highly negative to less negative. The red markers represent the Pareto front solutions, which highlight compositions with optimal trade-offs. Notably, in all three systems, the Pareto front points are concentrated toward the more negative current density regions, corresponding to better ORR performance.
- **Panel (b):** The similarity to the term ‘dielectric’ is shown. For all three systems, the Pareto-optimal points (red) exhibit lower similarity to ‘dielectric’, reflecting the requirement to minimize dielectric behavior for enhanced ORR activity. The Pareto front points are selected from the lower range of the similarity score distribution.

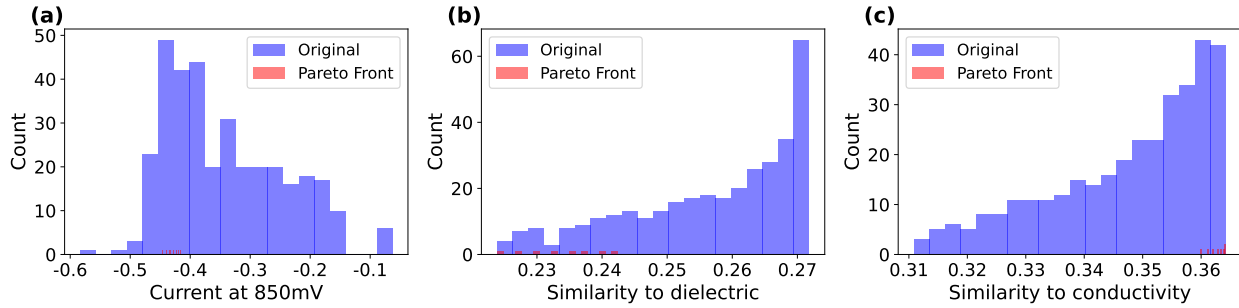


Figure 2: Measured current density distribution of AgPdPt system with their respective Pareto fronts highlighted: (a) current at 850 mV, (b) similarity to ‘dielectric’, and (c) similarity to ‘conductivity’.

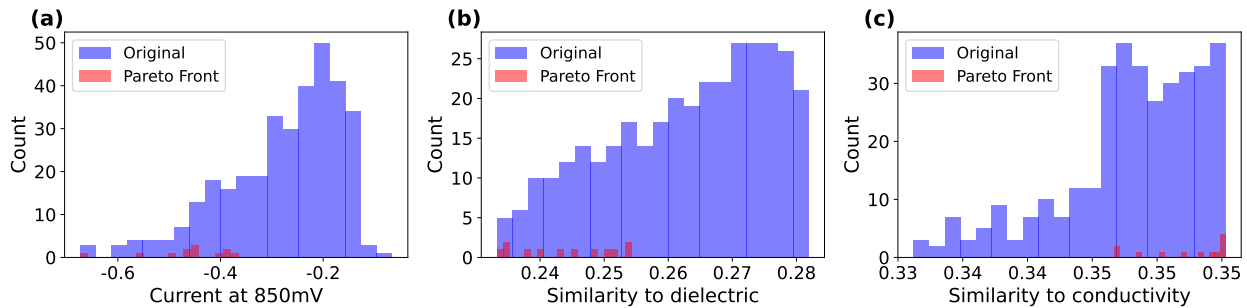


Figure 3: Measured current density distribution of AgPdRu system with their respective Pareto fronts highlighted: (a) current at 850 mV, (b) similarity to ‘dielectric’, and (c) similarity to ‘conductivity’.

- **Panel (c):** The similarity to ‘conductivity’ is shown. The Pareto front solutions show a higher similarity to ‘conductivity’, aligning with the need for materials with excellent conductive properties to support fast charge transfer during ORR. This trend is observed across all three systems, where the Pareto-optimal points lie toward the higher end of the similarity score distribution.

Fig. 5, 6, and 7 display the measured current density for the AgPdPt, AgPdRu, and AgPdPtRu systems, respectively, at 850 mV. X and y axes of the figures refer to real space coordinates of the location of measurements on a materials library – a thin film deposited on a wafer with approximately 10 cm diameter [46]. In each figure:

- **Panel (a):** This panel shows the reduced dataset after Pareto front calculation. The remaining points represent non-dominated solutions that balance the optimization objectives, highlighting the most promising compositions for ORR. By narrowing down the dataset, the Pareto front approach reduces the search space, focusing attention on the most relevant candidates for further investigation.

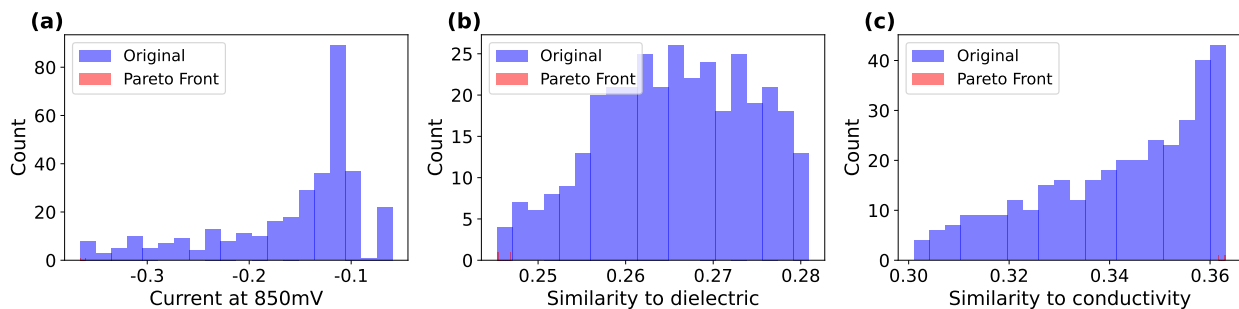


Figure 4: Measured current density distribution of AgPdPtRu system with their respective Pareto fronts highlighted: (a) current at 850 mV, (b) similarity to ‘dielectric’, and (c) similarity to ‘conductivity’.

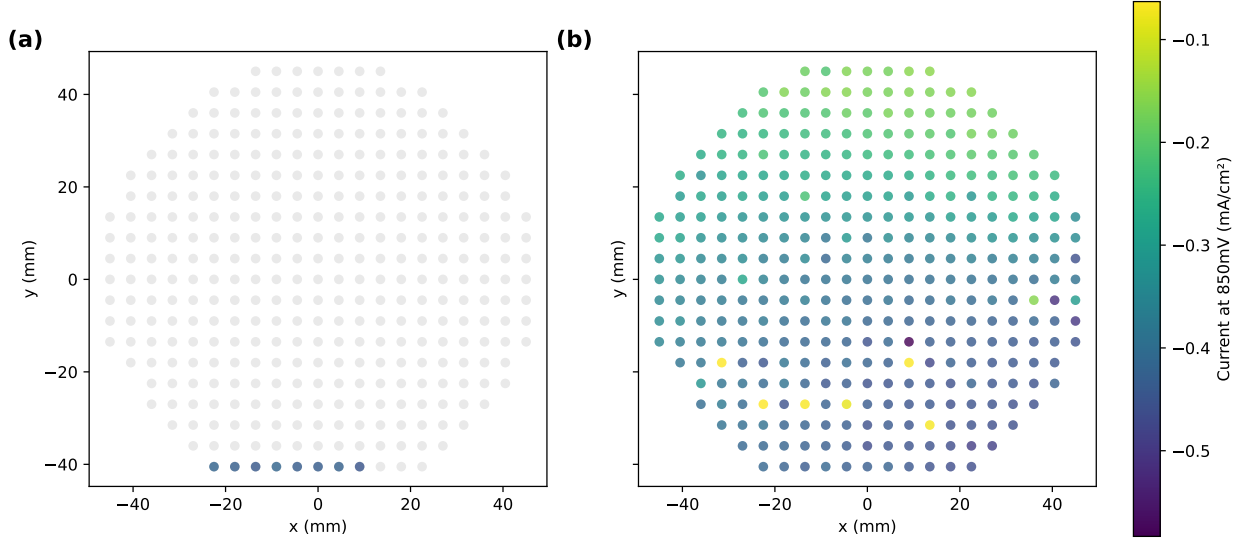


Figure 5: Measured current density for AgPdPt system: (a) High-performance predictions from Pareto front optimization highlighted and (b) original dataset with current density overlaid as color, more negative (blue) means better. Yellow locations are faulty measurements.

- **Panel (b):** Each point represents a specific material composition measured at an  $(x, y)$  coordinate on a wafer. The x-axis and y-axis correspond to physical locations on the wafer, with current density values at these positions color-coded according to the scale on the right. The color gradient ranges from less negative values (yellow and green) to more negative values (blue and purple), where more negative values indicate better ORR performance. Spatial variations in current density across the wafer reflect differences in material composition or testing conditions. Some isolated points with less negative current density appear within high-performance regions, potentially due to minor measurement errors. Hollow markers indicate positions excluded due to obvious test errors, such as near-zero current density, ensuring data reliability.

The results demonstrate that the Pareto front prediction effectively identifies high-performing compositions. This conclusion is validated by comparing the reduced dataset in Panel (a) to the original dataset in Panel (b), where high-performing candidates selected through the Pareto front approach correspond to regions of more negative current density.

Table 2 also compares the current density performance of the original and Pareto datasets. Key observations include:

- **AgPdPt:** The maximum current density improved from  $-0.063 \text{ mA/cm}^2$  (original) to  $-0.415 \text{ mA/cm}^2$  (Pareto), with a substantial reduction in standard deviation ( $0.098$  to  $0.011 \text{ mA/cm}^2$ ). This indicates a consistent high performance among Pareto-selected materials.
- **AgPdRu:** The Pareto dataset achieved a maximum current density of  $-0.364 \text{ mA/cm}^2$  compared to  $-0.065 \text{ mA/cm}^2$  in the original dataset, while retaining the same minimum value of  $-0.673 \text{ mA/cm}^2$ . The mean current density shifted closer to higher-performing candidates.
- **AgPdPtRu:** The maximum current density increased from  $-0.060 \text{ mA/cm}^2$  to  $-0.361 \text{ mA/cm}^2$ , with the standard deviation reduced to nearly zero ( $0.003 \text{ mA/cm}^2$ ), indicating strong agreement among selected candidates.

### 3.3 Results for HER Systems

#### 3.3.1 Elemental Composition

Table 1 highlights the elemental distribution in the HER systems. Notable trends include:

- In the AgAuPdPtRh system, the maximum concentration of Pt decreased slightly from 23 % to 21 %, while the minimum increased from 2 % to 5 %. This suggests that balanced Pt concentrations are associated with better-performing candidates.

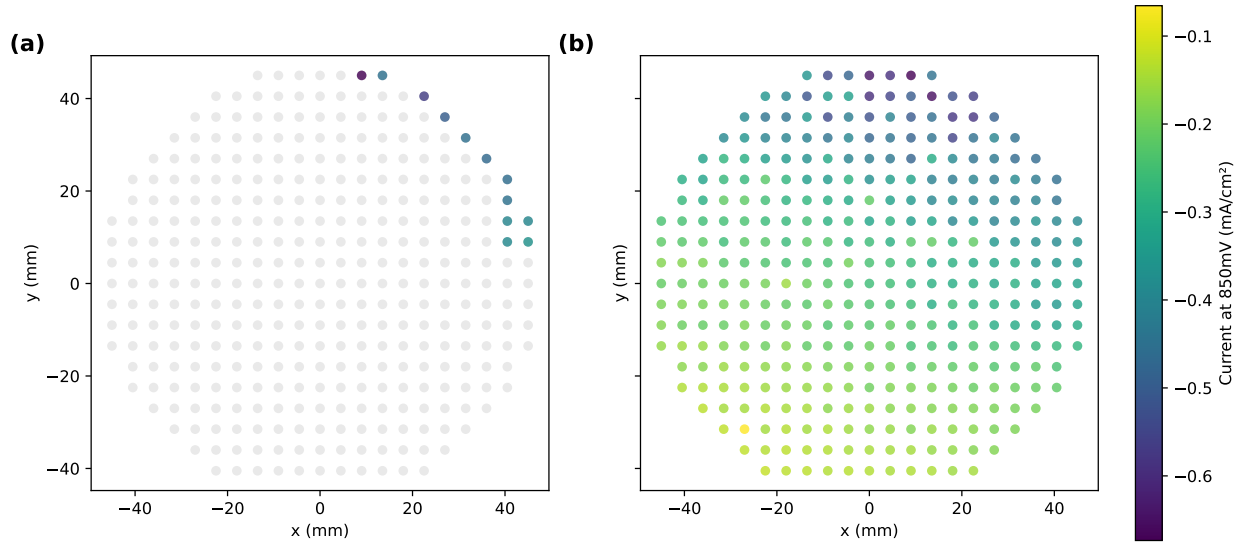


Figure 6: Like Fig. 5 but for the AgPdRu system.

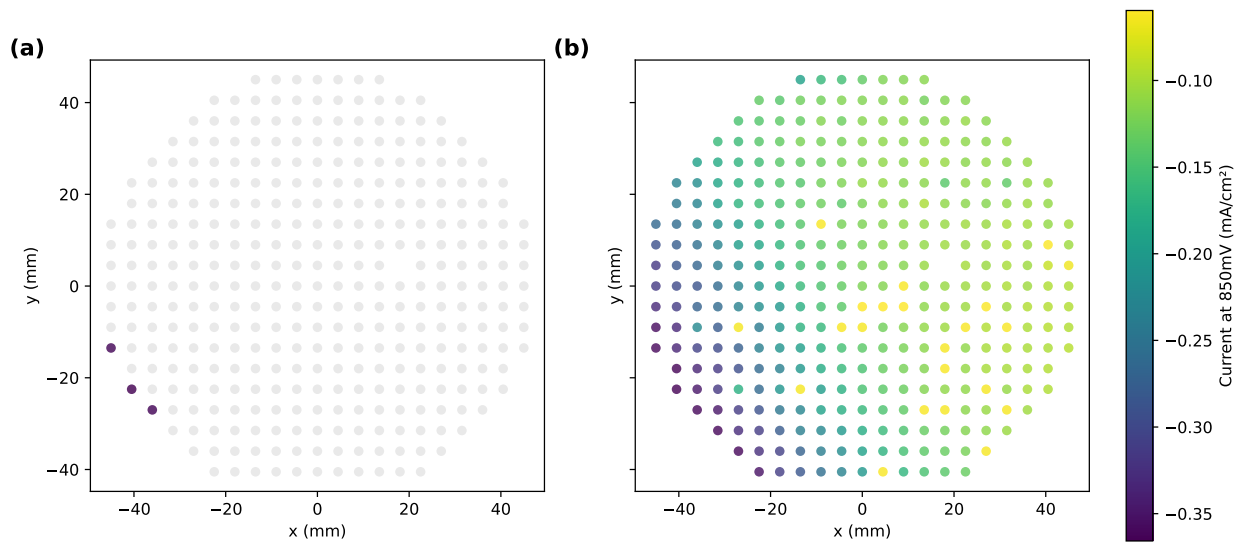


Figure 7: Like Fig. 5 but for AgPdPtRu system.

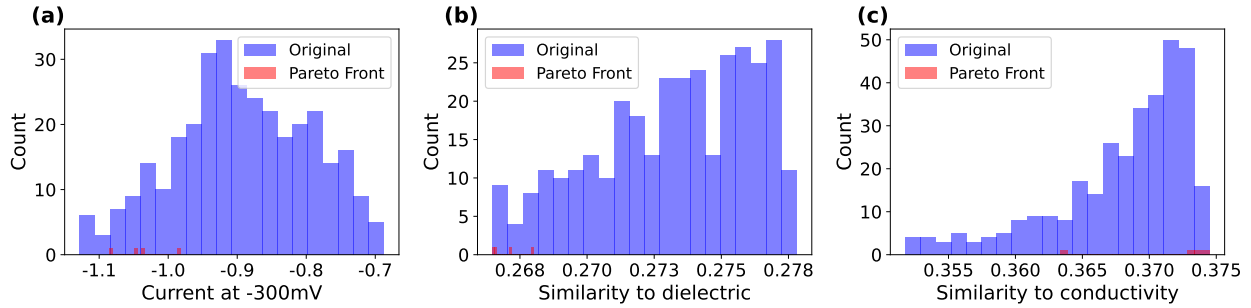


Figure 8: Measured current density distribution of AgAuPdPtRh system with their respective Pareto fronts highlighted: (a) current at -300 mV, (b) similarity to ‘dielectric’, and (c) similarity to ‘conductivity’.

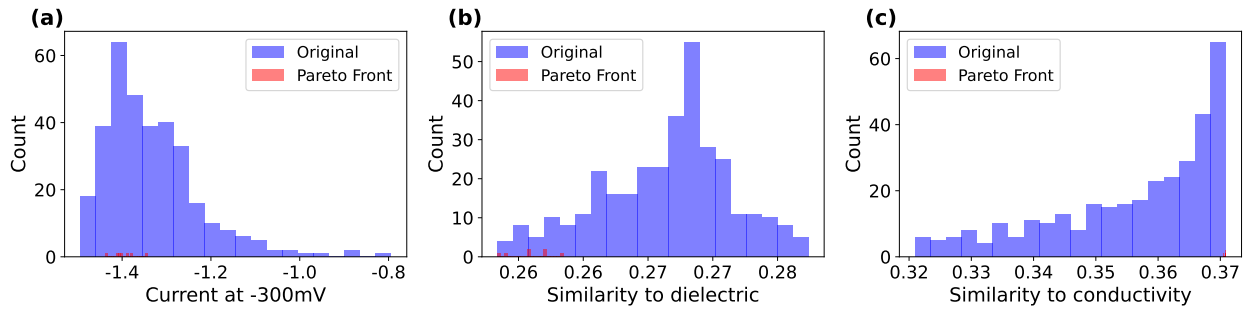


Figure 9: Measured current density distribution of AgAuPdPtRu system with their respective Pareto fronts highlighted: (a) current at -300 mV, (b) similarity to ‘dielectric’, and (c) similarity to ‘conductivity’.

- For AgAuPdPtRu, the maximum concentration of Ru decreased significantly from 61 % to 16 %, while the minimum concentration remained constant at 12 %. This indicates that excessively high Ru concentrations may not be favorable for HER under the given conditions.

### 3.3.2 Current Density Metrics

Fig. 8, 9 present the measured current density and similarity scores distribution for the AgAuPdPtRh and AgAuPdPtRu systems, respectively. For these two HER material systems, the Pareto front points are concentrated toward the more negative current density regions (Panel (a)) with lower similarity score to ‘dielectric’ (Panel (b)) and higher similarity score to ‘conductivity’ (Panel (c)).

Fig. 10 and 11 display the measured current density distribution after (Panel (a)) and before (Panel (b)) Pareto optimization for the AgAuPdPtRh and AgAuPdPtRu systems, respectively, at -300 mV, relevant to the HER.

Table 2 shows the current density performance before and after Pareto optimization. Key observations include:

- **AgAuPdPtRh:** The maximum current density improved from  $-0.688 \text{ mA/cm}^2$  (original) to  $-0.982 \text{ mA/cm}^2$  (Pareto). The standard deviation decreased from  $0.098$  to  $0.043 \text{ mA/cm}^2$ , indicating a consistently high performance among Pareto-selected materials.
- **AgAuPdPtRu:** The maximum current density improved significantly from  $-0.794 \text{ mA/cm}^2$  to  $-1.343 \text{ mA/cm}^2$ , with a reduction in standard deviation from  $0.107$  to  $0.030 \text{ mA/cm}^2$ . The mean current density shifted from  $-1.333$  to  $-1.395 \text{ mA/cm}^2$ , favoring higher-performing compositions.

## 3.4 Results for OER Systems

The experimental dataset is published on Zenodo [47].

### 3.4.1 Elemental Composition

Table 1 shows the elemental distribution for the OER system. Notable changes after Pareto optimization include:

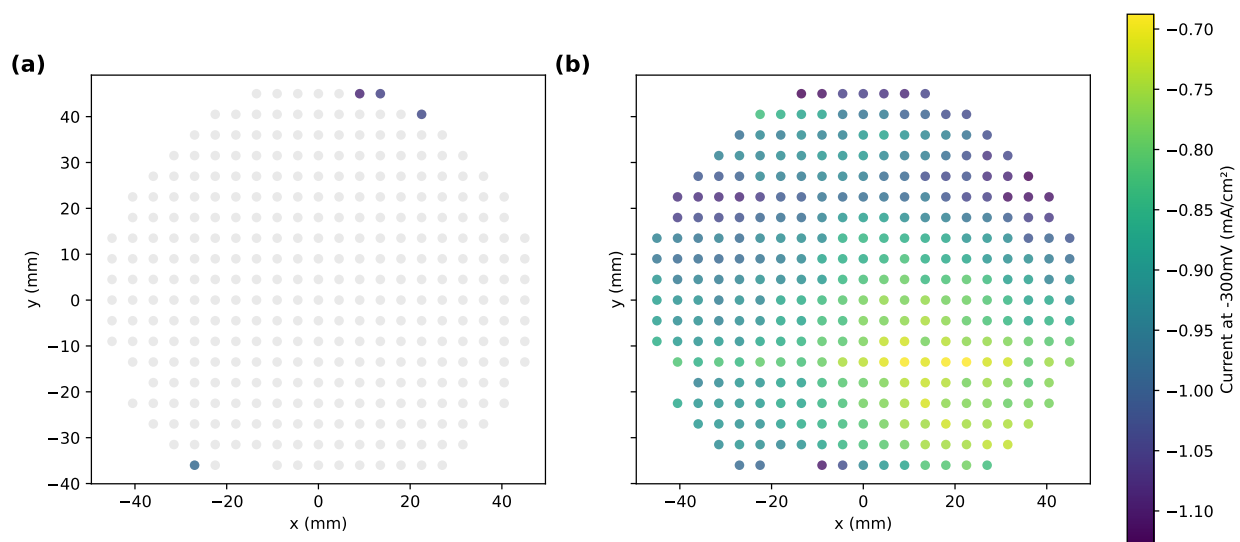


Figure 10: Like Fig. 5 but for the AgAuPdPtRh system.

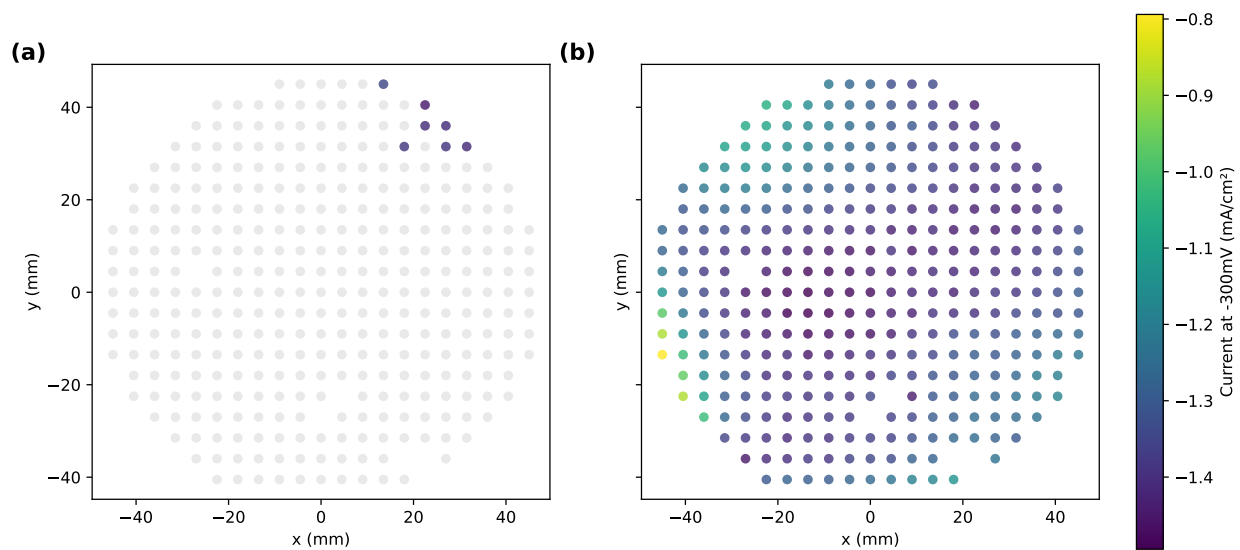


Figure 11: Like Fig. 5 but for the AgAuPdPtRu system.

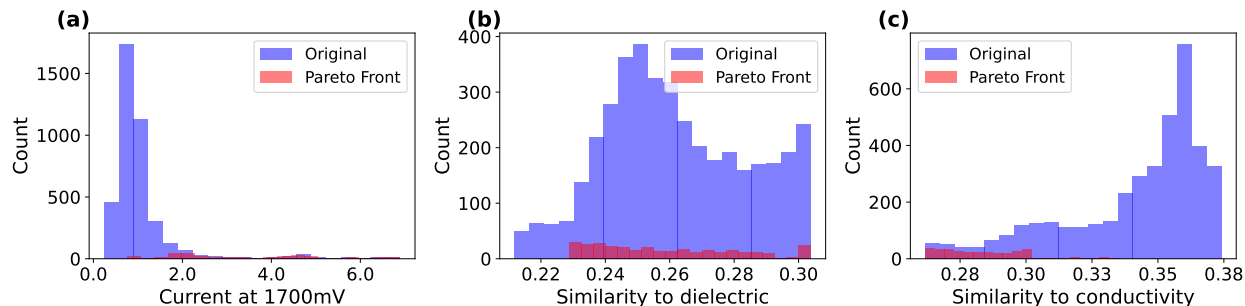


Figure 12: Measured current density distribution of NiPdPtRu system with their respective Pareto fronts highlighted: (a) current at 1700 mV, (b) similarity to ‘dielectric’, and (c) similarity to ‘conductivity’.

- The maximum concentration of Pt decreased drastically from 90% to 13%, and its minimum concentration remained at 0%. This indicates that lower Pt concentrations may be associated with higher-performing candidates under OER conditions.
- For Pd, the maximum concentration dropped from 89% to 10%, and its minimum concentration also remained at 0%. This trend mirrors that of Pt, suggesting a limited influence for Pd at high concentrations in OER performance.
- Ni concentrations were largely unchanged, with the maximum remaining at 80% and the minimum increasing slightly from 0% to 5%. This stability suggests that Ni plays a key role across a wide range of compositions.
- Ru concentrations showed the least variability, with the maximum remaining at 94% and the minimum increasing slightly from 0% to 8%.

### 3.4.2 Current Density Metrics

Fig. 12 shows the measured current density at 1700 mV and similarity scores distribution for the NiPdPtRu material system. The compositions selected through Pareto optimization are almost all distributed in higher current density region, which indicates better OER performance (Panel (a)), with high similarity score to ‘dielectric’ (Panel (b)) and low similarity score to ‘conductivity’ (Panel (c)).

Figure 13 shows the measured current density for the NiPdPtRu system at 1700 mV. In this system, data was collected from 12 individual experimental samples which span the composition range. Panel (a) displays the results after Pareto front calculation and Panel (b) shows the full data set across 12 individual samples. Individual subplots correspond to different wafers, illustrating the variations in current density due to compositional differences. Our method successfully identifies all the best-performing compositions which were measured on the sample displayed in the top right. This result demonstrates the method’s capability to effectively isolate high-performance candidates from a large dataset with spatial and compositional variations. All but the one identified sample show lower current density values.

As shown in Table 2 and Fig. 12, the performance of the NiPdPtRu system improved significantly after Pareto optimization:

- The mean current density increased from 1.073 mA/cm<sup>2</sup> (original) to 3.265 mA/cm<sup>2</sup> (Pareto), reflecting a shift toward higher-performing candidates.
- The minimum current density improved from 0.237 mA/cm<sup>2</sup> to 0.756 mA/cm<sup>2</sup>, further demonstrating the effectiveness of Pareto optimization.
- The standard deviation increased from 0.843 mA/cm<sup>2</sup> (original) to 1.633 mA/cm<sup>2</sup> (Pareto), indicating greater variability among the selected candidates, potentially due to the broader concentrations of elements in the original dataset.

## 4 Discussion

Our approach, which combines text mining, word embedding-based representations of compositions and properties in conjunction with Pareto front optimization, demonstrates its effectiveness by systematically narrowing down high-performing composition candidates from large compositional spaces with a very fine resolution in individual element

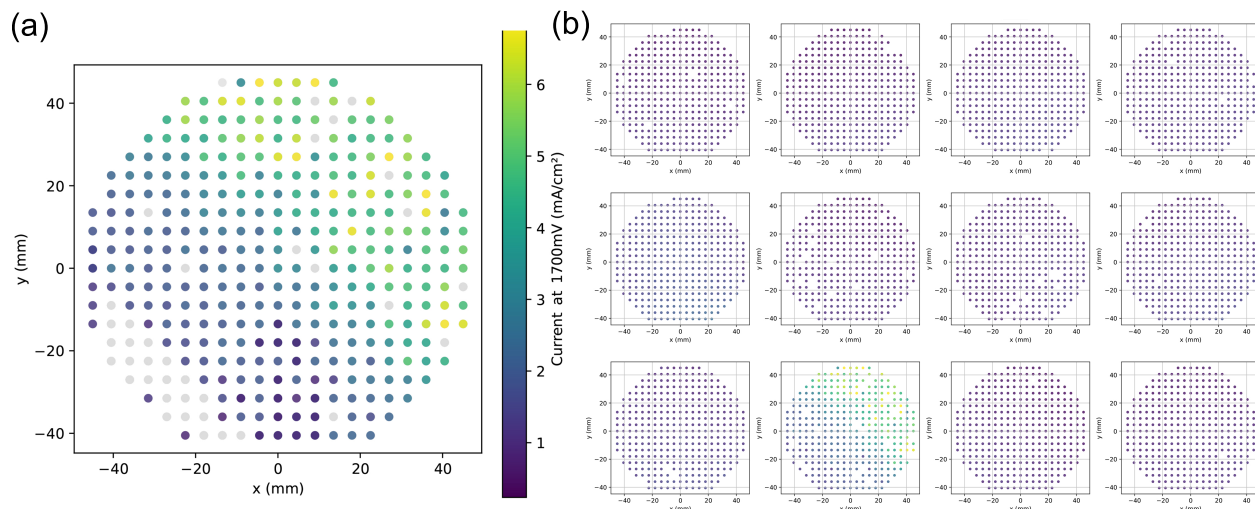


Figure 13: Measured current density for the NiPdPtRu system: (a) High-performance predictions from Pareto front optimization highlighted and (b) original dataset spread across 12 experimental samples with current density overlaid as color, more positive (yellow) means better.

concentrations at the level of single percentage changes. We automate the extraction of materials-relevant information from scientific literature, transforming qualitative descriptions into quantitative metrics. The use of word embeddings to represent materials and their properties, such as conductivity and dielectric behavior, allows us to evaluate candidate compositions w.r.t. their experimentally-measured performance. Our method provides a tool to significantly reduce the experimental workload by focusing on compositions which are likely to meet specific performance criteria. Compared to trial-and-error approaches and even high-throughput screening, our strategy accelerates the identification of promising materials for electrocatalytic applications, offering a scalable framework that bridges data science and materials discovery and optimization and thereby directly addresses the problem of the ‘combinatorial explosion’.

However, there are several assumptions in our approach which warrant further discussion. First, we assume that the multi-element compositions can be represented as a weighted linear combination of single-element representations. The main reason to linearly combine single-element representations is that almost none of the specific compositions for compositionally complex solid solutions have been measured experimentally and subsequently reported. This is in contrast and the main difference to the one-hot encoding of materials with several elements, e.g. [36] where materials like  $\text{Bi}_2\text{Te}_3$  receive their own embedding. In our approach, individual elements – Bi and Te in this example – are individually encoded. Thereby, we open up the representation space for arbitrary compositions which have not been explicitly reported in literature. While this approximation is computationally straightforward to represent arbitrary compositions, it does not account for potential non-linear effects or complex interactions between elements. Given the success of our approach, we assume that possible non-linear relationships are to some extent taken care of by the high dimensionality (200) of our embedding space. Linearly combining individual elements’ representations for arbitrary composition consequently also implies that composition-property relationships are smooth in the high-dimensional embedding space. We argue that this is a valid assumption since many material properties vary comparatively smoothly with composition.

Second, the use of similarity scores for ‘conductivity’ and ‘dielectric’ as optimization objectives is based on the known requirements for specific electrochemical reactions (e.g., high conductivity for ORR and HER, high dielectric for OER). This assumption is based on domain knowledge and does not generalize to other applications without modification. In other words, the similarity scores with specific materials properties as descriptors for reaction-specific performance predictions can be seen as domain knowledge informed *lucky guesswork*. For other reactions or material classes or even completely other problems, alternative target properties (‘descriptors’) must be identified based on experimental insights or theoretical considerations.

Lastly, Pareto front optimization is to identify high-performance candidate compositions. While the current implementation demonstrates the flexibility of Pareto optimization, additional objectives such as stability, cost, or scalability could be included to refine the predictions further. Different multi-objective optimization strategies could also be explored to better tailor the results for specific reactions or material systems.

By addressing these assumptions and exploring potential refinements, the proposed framework can be extended to a broader range of materials discovery and design challenges to include more constraints. The results presented here highlight the power of integrating latent knowledge in scientific texts with an optimization algorithm, showcasing a path toward data-driven, data-efficient exploration of complex compositional spaces where little prior data, specifically application-relevant data, exists.

#### 4.1 Comparison Across Reactions

The analysis of ORR, HER, and OER systems highlights the effectiveness of combining text mining, word embeddings, and Pareto optimization to identify high-performance electrocatalysts reliably without any prior knowledge about their electrocatalytic performance. Each reaction requires a different strategy. This section discusses the broader implications of the observed trends.

- **ORR systems:** Narrower ranges of Pt and Pd concentrations were observed, indicating a need for balanced compositions to optimize catalytic activity. This reflects the importance of synergy between these elements for efficient oxygen reduction.
- **HER systems:** Moderate concentrations of Ru and Pt were favored, while excessively high concentrations were filtered out. This suggests that a balanced distribution of these key elements is more effective for HER than a high concentration of a single element in large amounts, likely because balanced compositions provide a better environment for catalytic activity across the composition space.
- **OER systems:** The broader range of Ni and Ru concentrations retained after optimization suggests that OER can tolerate diverse compositions. This may indicate that the performance of OER systems is less dependent on precise elemental ratios and more on the overall presence of these active elements.

These trends demonstrate that elemental composition preferences are reaction-specific, emphasizing the importance of tailoring optimization objectives to the unique electrochemical demands of each reaction [22, 23, 24, 25].

#### 4.2 Role of Text Mining and Word Embeddings in Optimization

Text mining and word embeddings provided a systematic way to incorporate material representations into an optimization or discovery process. By processing scientific abstracts, text mining extracted relevant terms and relationships that are often scattered across literature. Word embeddings transform these terms into numerical representations, making it possible to calculate similarity metrics for properties like conductivity and dielectric behavior and derive meaningful, reaction-specific descriptors. Combined with our linear mixing approach for the composition, this opens up the search of the entire compositions space.

These similarity metrics with materials properties play a key role in guiding the optimization. For example, in ORR and HER systems, the similarity to conductivity terms help identify materials with electronic properties suited for fast charge transfer. Conversely, in OER systems, the similarity to dielectric terms favors materials more aligned with its electronic requirements. We demonstrated how this process translates qualitative descriptions of materials into quantitative metrics, to filter high performance candidate compositions in large search spaces with high compositional resolution.

The use of text-derived similarities aligns well with the broader goal of electrocatalyst discovery: connecting material compositions and their expected properties to performance metrics in a systematic way. However, the reliance on embeddings derived solely from textual descriptions also raises questions about the completeness of the data, as some material properties might not be explicitly mentioned in the abstracts.

#### 4.3 Challenges and Next Steps

Despite our demonstrated success, our approach has room for improvement:

- **Data Quality:** The quality of the results depends on the quality of the initial text corpus. Missing or biased data can affect the embeddings and the optimization process. We are currently exploring strategies for strategic corpus-building. This will be published in a separate contribution.
- **Balancing Objectives:** Defining the correct optimization goals and weights requires expertise and it is yet unclear how to formalize this process beyond our “lucky guess”.

## 5 Conclusions

Our study outlines an approach for discovering high-performance electrocatalyst materials using automated text mining, Word2Vec models, and Pareto front analysis with high resolution in composition space where experimental data is usually scarce. Pareto optimization is used to refine large datasets with many candidate compositions into smaller, focused collections of potentially high-performing candidates, tailored to the unique requirements of oxygen reduction (ORR), hydrogen evolution (HER), and oxygen evolution (OER) reactions. Validated on multiple experimentally-measured datasets, our method reliably identifies compositions with high performance, significantly reducing the candidate pool markedly while maintaining strong property correlations.

## Author Contributions

**Lei Zhang:** Conceptualization, Methodology, Software, Validation, Formal analysis, Investigation, Data Curation, Writing - Original Draft, Visualization, Experimentation, Funding acquisition.

**Markus Stricker:** Conceptualization, Resources, Supervision, Writing - Review & Editing.

## Conflicts of interest

There are no conflicts to declare.

## Acknowledgements

Both authors gratefully acknowledge the financial support provided by the China Scholarship Council (CSC, CSC number: 202208360048), which is instrumental in facilitating this research. The authors express their gratitude to Lars Banko, Wolfgang Schuhmann, and Alfred Ludwig for their invaluable experimental support and for providing the data used to validate the prediction results. Additionally, the authors acknowledge funding by the Deutsche Forschungsgemeinschaft (DFG, German Research Foundation) through CRC 1625, project number 506711657, subprojects INF, A05.

## References

- [1] Rod Borup, Jeremy Meyers, Bryan Pivovar, Yu Seung Kim, Rangachary Mukundan, Nancy Garland, Deborah Myers, Mahlon Wilson, Fernando Garzon, David Wood, Piotr Zelenay, Karren More, Ken Stroh, Tom Zawodzinski, James Boncella, James E. McGrath, Minoru Inaba, Kenji Miyatake, Michio Hori, Kenichiro Ota, Zempachi Ogumi, Seizo Miyata, Atsushi Nishikata, Zyun Siroma, Yoshiharu Uchimoto, Kazuaki Yasuda, Ken-Ichi Kimijima, and Norio Iwashita. Scientific aspects of polymer electrolyte fuel cell durability and degradation. *Chemical Reviews*, 107(10):3904 – 3951, 2007. Cited by: 3092.
- [2] Mark K. Debe. Electrocatalyst approaches and challenges for automotive fuel cells. *Nature*, 486(7401):43 – 51, 2012. Cited by: 4978.
- [3] Michel Lefèvre, Eric Proietti, Frédéric Jaouen, and Jean-Pol Dodelet. Iron-based catalysts with improved oxygen reduction activity in polymer electrolyte fuel cells. *Science*, 324(5923):71 – 74, 2009. Cited by: 2899.
- [4] Ryan J. R. Jones, Yungchieh Lai, Dan Guevarra, Kevin Kan, Joel A. Haber, and John M. Gregoire. Accelerated screening of gas diffusion electrodes for carbon dioxide reduction. *Digital Discovery*, 3(6):1144 – 1149, 2024. Cited by: 1; All Open Access, Gold Open Access.
- [5] Shahid Zaman, Mohmmad Khalid, and Samaneh Shahgaldi. Advanced electrocatalyst supports for proton exchange membrane water electrolyzers. *ACS Energy Letters*, 9(6):2922 – 2935, 2024. Cited by: 7.
- [6] Jyoti Ranjan Mandal, Khushboo Singh, and Vinod K. Shahi. Amphoteric membrane loaded with a noble metal-free hollow spherical nicop@rgo bifunctional electrocatalyst for alkaline water electrolyzers. *ACS Applied Energy Materials*, 5(7):8611 – 8620, 2022. Cited by: 8.
- [7] Tsuyohiko Fujigaya, Yilei Shi, Jun Yang, Hua Li, Kohei Ito, and Naotoshi Nakashima. A highly efficient and durable carbon nanotube-based anode electrocatalyst for water electrolyzers. *Journal of Materials Chemistry A*, 5(21):10584 – 10590, 2017. Cited by: 21.
- [8] Jadranka Milikić, Ana Nastasić, Marta Martins, César A. C. Sequeira, and Biljana Šljukić. Air cathodes and bifunctional oxygen electrocatalysts for aqueous metal–air batteries. *Batteries*, 9(8):394, 2023. Cited by: 13; All Open Access, Gold Open Access.

- [9] Manuel Salado and Erlantz Lizundia. Advances, challenges, and environmental impacts in metal–air battery electrolytes. *Materials Today Energy*, 28:101064, 2022. Cited by: 55; All Open Access, Hybrid Gold Open Access.
- [10] Lei Ye, Yang Hong, Meng Liao, Bingjie Wang, Dacheng Wei, and Huisheng Peng. Recent advances in flexible fiber-shaped metal-air batteries. *Energy Storage Materials*, 28:364 – 374, 2020. Cited by: 96.
- [11] Michael J. Statt, Brian A. Rohr, Kris Brown, Dan Guevarra, Jens Hummelshøj, Linda Hung, Abraham Anapolsky, John M. Gregoire, and Santosh K. Suram. Esamp: event-sourced architecture for materials provenance management and application to accelerated materials discovery. *Digital Discovery*, 2(4):1078 – 1088, 2023. Cited by: 3; All Open Access, Gold Open Access.
- [12] Kuanping Gong, Feng Du, Zhenhai Xia, Michael Durstock, and Liming Dai. Nitrogen-doped carbon nanotube arrays with high electrocatalytic activity for oxygen reduction. *Science*, 323(5915):760 – 764, 2009. Cited by: 6612.
- [13] Keiichi Okubo, Jaydeep Thik, Tomoya Yamaguchi, and Chen Ling. Computer vision enabled high-quality electrochemical experimentation. *Digital Discovery*, 3(11):2183 – 2191, 2024. Cited by: 0; All Open Access.
- [14] Savannah Talledo, Andrew Kubaney, Mitchell A. Baumer, Keegan Pietrak, and Stefan Bernhard. High throughput methodology for investigating green hydrogen generating processes using colorimetric detection films and machine vision. *Digital Discovery*, 3(7):1430 – 1440, 2024. Cited by: 0; All Open Access, Gold Open Access.
- [15] Jeff Greeley, Thomas F. Jaramillo, Jacob Bonde, Ib Chorkendorff, and Jens K. Nørskov. Computational high-throughput screening of electrocatalytic materials for hydrogen evolution. *Nature Materials*, 5(11):909 – 913, 2006. Cited by: 3423.
- [16] Jehad Abed, Yang Bai, Daniel Persaud, Jiheon Kim, Julia Witt, Jason Hattrick-Simpers, and Edward H. Sargent. Ampere: automated modular platform for expedited and reproducible electrochemical testing. *Digital Discovery*, 3(11):2265 – 2274, 2024. Cited by: 0; All Open Access.
- [17] Charles C. L. McCrory, Suho Jung, Jonas C. Peters, and Thomas F. Jaramillo. Benchmarking heterogeneous electrocatalysts for the oxygen evolution reaction. *Journal of the American Chemical Society*, 135(45):16977 – 16987, 2013. Cited by: 5467; All Open Access, Green Open Access.
- [18] Thomas A.A. Batchelor, Jack K. Pedersen, Simon H. Winther, Ivano E. Castelli, Karsten W. Jacobsen, and Jan Rossmeisl. High-entropy alloys as a discovery platform for electrocatalysis. *Joule*, 3(3):834 – 845, 2019. Cited by: 569; All Open Access, Bronze Open Access.
- [19] Ridha Zerdoumi, Alfred Ludwig, and Wolfgang Schuhmann. High entropy intermetallic compounds: A discovery platform for structure–property correlations and materials design principles in electrocatalysis. *Current Opinion in Electrochemistry*, 48:101590, 2024.
- [20] Aamar F. Khan, Edward P. Randviir, Dale A. C. Brownson, Xiaobo Ji, Graham C. Smith, and Craig E. Banks. 2d hexagonal boron nitride (2d-hbn) explored as a potential electrocatalyst for the oxygen reduction reaction. *Electroanalysis*, 29(2):622 – 634, 2017. Cited by: 46; All Open Access, Hybrid Gold Open Access.
- [21] SK Safdar Hossain, Syed Sadiq Ali, Sayeed Rushd, Bamidele Victor Ayodele, and Chin Kui Cheng. Interaction effect of process parameters and pd-electrocatalyst in formic acid electro-oxidation for fuel cell applications: Implementing supervised machine learning algorithms. *International Journal of Energy Research*, 46(15):21583 – 21597, 2022. Cited by: 11; All Open Access, Gold Open Access.
- [22] Anuj Kumar, Shashank Sundriyal, Charu Goyal, Tribani Boruah, Dipak Kumar Das, Ghulam Yasin, Tuan Anh Nguyen, and Sonali Gautam. *Metal-organic frameworks for the electrocatalytic ORR and HER*. Micro and Nano Technologies, 2022. Cited by: 4.
- [23] S.S. Shinde, Abdul Sami, and Jung-Ho Lee. Lanthanides-based graphene catalysts for high performance hydrogen evolution and oxygen reduction. *Electrochimica Acta*, 214:173 – 181, 2016. Cited by: 23.
- [24] Shuang Wang, Qiong Li, Shujuan Sun, Kai Ge, Yi Zhao, Kai Yang, Zhiheng Zhang, Jiayu Cao, Jie Lu, Yongfang Yang, Yue Zhang, Mingwang Pan, Zhiqun Lin, and Lei Zhu. Heterostructured ferroelectric batio<sub>3</sub>@mof-fe/ co electrocatalysts for efficient oxygen evolution reaction. *Journal of Materials Chemistry A*, 10(10):5350 – 5360, 2022. Cited by: 26.
- [25] Nguyen Thi Thu Thao, Kwangsoo Kim, Jeong Ho Ryu, Byeong-Seon An, Arpan Kumar Nayak, Jin Uk Jang, Kyeong-Han Na, Won-Youl Choi, Ghulam Ali, Keun Hwa Chae, Muhammad Akbar, Kyung Yoon Chung, Hyun-Seok Cho, Jong Hyeok Park, Byung-Hyun Kim, and HyukSu Han. Colossal dielectric perovskites of calcium copper titanate (cacu<sub>3</sub>ti<sub>4</sub>o<sub>12</sub>) with low-iridium dopants enables ultrahigh mass activity for the acidic oxygen evolution reaction. *Advanced Science*, 10(16):2207695, 2023. Cited by: 10; All Open Access, Gold Open Access.

- [26] Lei Zhang, Juntong Huang, Zhihui Hu, Xibao Li, Tianyi Ding, Xifeng Hou, Zhi Chen, Zhiguo Ye, and Ruiying Luo. Ni(no3)<sub>2</sub>-induced high electrocatalytic hydrogen evolution performance of self-supported fold-like wc coating on carbon fiber paper prepared through molten salt method. *Electrochimica Acta*, 422:140553, 2022.
- [27] Zhi Wei She, Jakob Kibsgaard, Colin F. Dickens, Ib Chorkendorff, Jens K. Nørskov, and Thomas F. Jaramillo. Combining theory and experiment in electrocatalysis: Insights into materials design. *Science*, 355(6321):ead4998, 2017. Cited by: 7528; All Open Access, Green Open Access.
- [28] Tobias Löffler, Alfred Ludwig, Jan Rossmeis, and Wolfgang Schuhmann. What makes high-entropy alloys exceptional electrocatalysts? *Angewandte Chemie International Edition*, 60(52):26894–26903, 2021.
- [29] Markus Stricker, Lars Banko, Nik Sarazin, Niklas Siemer, Jan Janssen, Lei Zhang, Jörg Neugebauer, and Alfred Ludwig. Computationally accelerated experimental materials characterization – drawing inspiration from high-throughput simulation workflows, 2025.
- [30] Ge Lei, Ronan Docherty, and Samuel J. Cooper. Materials science in the era of large language models: a perspective. *Digital Discovery*, 3(7):1257 – 1272, 2024. Cited by: 0; All Open Access, Gold Open Access.
- [31] Arun Muthukkumaran, Shrayas Raghunathan, Arjun Ravichandran, and Raghunathan Rengaswamy. Perovskite-based electrocatalyst discovery and design using word embeddings from retrained scibert language model. *AICHE Journal*, 69(7):e18068, 2023. Cited by: 2.
- [32] Jianwen Liu, Wenzhi Luo, Lei Wang, Jiujuan Zhang, Xian-Zhu Fu, and Jing-Li Luo. Toward excellence of electrocatalyst design by emerging descriptor-oriented machine learning. *Advanced Functional Materials*, 32(17):2110748, 2022. Cited by: 62.
- [33] Letian Chen, Yun Tian, Xu Hu, Sai Yao, Zhengyu Lu, Suya Chen, Xu Zhang, and Zhen Zhou. A universal machine learning framework for electrocatalyst innovation: A case study of discovering alloys for hydrogen evolution reaction. *Advanced Functional Materials*, 32(47):2208418, 2022. Cited by: 51.
- [34] Haoxin Mai, Tu C. Le, Dehong Chen, David A. Winkler, and Rachel A. Caruso. Machine learning for electrocatalyst and photocatalyst design and discovery. *Chemical Reviews*, 122(16):13478 – 13515, 2022. Cited by: 201.
- [35] Lei Zhang and Markus Stricker. Matnexus: A comprehensive text mining and analysis suite for materials discovery. *SoftwareX*, 26:101654, 2024. Cited by: 0; All Open Access, Green Open Access.
- [36] Vahe Tshitoyan, John Dagdelen, Leigh Weston, Alexander Dunn, Ziqin Rong, Olga Kononova, Kristin A. Persson, Gerbrand Ceder, and Anubhav Jain. Unsupervised word embeddings capture latent knowledge from materials science literature. *Nature*, 571(7763):95–98, July 2019.
- [37] Lei Zhang and Markus Stricker. Repository for ‘electrocatalyst discovery through text mining and multi-objective optimization’. [https://github.com/lab-mids/word\\_embedding\\_pareto\\_front](https://github.com/lab-mids/word_embedding_pareto_front), 2025.
- [38] Tomas Mikolov, Kai Chen, Greg Corrado, Jeffrey Dean, L Sutskever, and Geoffrey Zweig. word2vec. *URL* <https://code.google.com/p/word2vec/>, 22:795, 2013.
- [39] Yoav Goldberg and Omer Levy. word2vec explained: deriving mikolov et al.’s negative-sampling word-embedding method, 2014.
- [40] Anna Rogers, Olga Kovaleva, and Anna Rumshisky. A primer in bertology: What we know about how bert works. *Transactions of the Association for Computational Linguistics*, 8:842 – 866, 2020. Cited by: 815; All Open Access, Gold Open Access.
- [41] Lucas Foppa, Luca M. Ghiringhelli, Frank Girgsdies, Maike Hashagen, Pierre Kube, Michael Hävecker, Spencer J. Carey, Andrey Tarasov, Peter Kraus, Frank Rosowski, Robert Schlögl, Annette Trunschke, and Matthias Scheffler. Materials genes of heterogeneous catalysis from clean experiments and artificial intelligence. *MRS Bulletin*, 46(11):1016 – 1026, 2021. Cited by: 35; All Open Access, Hybrid Gold Open Access.
- [42] Vilfredo Pareto. *Cours d’économie politique*. F. Rouge, 1896.
- [43] F. Djeflal and N. Lakhdar. An improved analog electrical performance of submicron dual-material gate (dm) gaas-mesfets using multi-objective computation. *Journal of Computational Electronics*, 12(1):29 – 35, 2013. Cited by: 32.
- [44] Ashwin A. Bale, Sachin M. B. Gautham, and Tarak K. Patra. Sequence-defined pareto frontier of a copolymer structure. *Journal of Polymer Science*, 60(14):2100 – 2113, 2022. Cited by: 6; All Open Access, Green Open Access.
- [45] Lars Banko, Olga Krysiak, Wolfgang Schumann, and Alfred Ludwig. Electrochemical activity of several compositions in the system ag-pd-pt-ru for the oxygen reduction reaction in 0.05 m koh solution ph 12.5, October 2024.

- [46] Alfred Ludwig. Discovery of new materials using combinatorial synthesis and high-throughput characterization of thin-film materials libraries combined with computational methods. *npj Computational Materials*, 5(1):70, 2019.
- [47] Felix Thelen, Rico Zehl, Ridha Zerdoumi, Jan Lukas Bürgel, Wolfgang Schuhmann, and Alfred Ludwig. Dataset - accelerating combinatorial electrocatalyst discovery with bayesian optimization: A case study in the quaternary system ni-pd-pt-ru for the oxygen evolution reaction, February 2025.